Collision Spectroscopy of Highly Charged Ions at the ESR Storage Ring *

Th. Stöhlker

Institut für Kernphysik, Universität Frankfurt, August-Euler-Straße 2, 60486 Frankfurt, Germany and GSI, Planckstraße 1, 62491 Darmstadt, Germany

(February 3, 1999)

With the advent of the relativistic storage ring ESR, a new generation of highly precise collision experiments has become accessible even for the heaviest ion species. At the ESR, the interaction of brilliant beams of cooled high-Z ions with low-dense gaseous matter can be studied without any beam collimation guaranteeing background-free experimental conditions. Furthermore, a unique feature of the ring is its capability to decelerate even bare uranium ions to moderate energies close to about 10 MeV/u, i.e. it allows to scan the beam energies from highly relativistic encounters to almost slow collisions. Currently, the main experimental activities focus on final state resolved electron capture, photon angular distribution and alignment investigations.

34.70.+e, 31.30.Jv, 31.50.+w, 32.80.-t

I. INTRODUCTION

For atomic collision physics dealing with relativistic heavy-ion beams, a unique tool has become available with the advent of the heavy-ion storage ring ESR at GSI in Darmstadt [1–3]. At the ESR almost all ion species up to bare uranium can be accumulated, stored and cooled by electrons. The electron cooling technique guarantees for brilliant high intensity beams, with precisely known energies, charge states, momentum spread and beam diameters close to 1 mm. Along with the internal jet target available at the ESR [4], where

*Dedicated to Prof. Horst Schmidt Böcking on the occasion of his 60^{th} birthday.

thin gaseous targets from H_2 up to Xe can be used, the interaction of these beams with matter can be studied under single collision condition ($\rho \approx 10^{12}$p/cm^3). Most important and in contrast to conventional single-pass experiments where direct beams from relativistic accelerators are used, no active or passive beam collimation is required at the ESR. Thus, experimental conditions are almost completely background-free. A further important feature of the ESR must be stressed: the deceleration capability of the storage ring which allows one to investigate the dynamics in ion-atom collisions over a wide range of energies [5].

Until now most experiments conducted at the jet target of the ring concentrated on QED investigations for high-Z one-electron ions [3]. However, by means of x-ray spectroscopy, a few dedicated atomic collision experiments could already be performed for high-Z ions. Here, exclusive electron capture studies and the investigation of the time-reversed photoeffect were addressed, fields of research which are now accessible for the first time by experiments. Moreover, also the topics of K-shell Coulomb excitation [6], simultaneous excitation and ionization of high-Z He-like ions [7], electron bremsstrahlung [8], correlated two-electron capture [9] are currently under investigation.

In the following, a short overview over the current status of the atomic collision experiments at the ESR will be given thereby concentrating on one-electron capture processes occurring in collisions of high-Z projectiles and gaseous matter.

II. ELECTRON CAPTURE STUDIES

One of the most basic processes in atomic collision physics is the transfer of an electron between a target and a fast moving ion. In the nonrelativistic collision domain, where $\beta \ll 1$ (β denotes the projectile velocity v in units of speed of light c), this process is entirely governed by the so-called *nonradiative electron capture* process (NRC), where the energy and momentum transfer in the collision is shared between the projectile, target, and the captured electron. Already from the historically first theory for NRC, the Oppenheimer-Brinkman-Kramers approach (OBK) [10], it is known, that this process possesses a dramatic velocity dependence which approaches asymptotically v^{-12} or E^{-6}. Also, its cross section follows a strong dependence on the projectile and target atomic charge numbers (Z_P and Z_T) which scales like

$$\sigma_{NRC} \propto \frac{Z_T^5 \times Z_P^5}{v^{12}}. \tag{1}$$

Although, in the ultra-relativistic limit the correct asymptotic energy dependence of σ_{NRC} is given by E^{-1}, this process practically plays no role at relativistic encounters ($\beta > 0.5$) of heavy, highly charged ions and low-Z target atoms. Since high energies are required for an effective production of high charge states [11,12], no experimental cross-section data were available for bare or even few-electron, high-Z ions colliding with atoms far below the ion production energy. However, such data are most important since they are in particular sensitive to Coulomb distortion effects which are most difficult to describe theoretically (for a detailed discussion see e.g. [11]). Contrary, at highly energetic collisions, electron transfer is entirely determined by *radiative electron capture* (REC), where the coupling between the electron and the electromagnetic field of the moving ion results in an electron capture via simultaneous emission of a photon carrying away the energy and momentum difference between the initial and final electron states. Within the impulse approximation, REC can be considered as the time-reversed photoionization [13–16]. The general scaling properties of REC can already be derived from the nonrelativistic dipole-approximation of Stobbe and are given by:

$$\sigma_{REC} \propto \frac{Z_T \times Z_P^5}{v^{5/2}}. \tag{2}$$

The discussed interplay between both capture processes, REC and NRC, is depicted in Fig. 1, where the measured electron capture cross-sections for $U^{92+} \rightarrow N_2$ collisions are given for relativistic encounters (220 and 358 MeV/u) as well as for almost slow collisions (49 and 68 MeV/u) [5]. The latter were obtained by exploiting the deceleration capability of the ESR storage ring. In addition, the experimental data (solid circles) are compared with a theoretical calculation (full line) based on the relativistic eikonal approximation for NRC (dashed line) [17,18], an accessible distorted-wave theory, which, in its asymmetric form, approximately includes the Coulomb distortion in one of the entrance or exit channels. Here, we applied the higher-potential prescription as discussed in Ref. [11,17] . Also REC was taken into account by using the nonrelativistic dipole approximation [13] which is known to describe reasonably well total REC cross sections due to an accidental cancellation between various relativistic effects [16]. As seen in the figure, an excellent agreement between the experimental results and the theoretical predictions can be stated. We believe, that the excellent agreement, in particular at low energies, is fortuitous, since the eikonal approximation is known to predict absolute cross-section values within a factor of two. In addition, we performed NRC calculations on the ground of the *continuum distorted wave approximation* (CDW) [19] which satisfies the Coulomb boundary conditions, most desirable when dealing with NRC. Since, the calculation was performed by means of an nonrelativistic code, we restrict the comparison to the two lowest energies (see open triangles). Again, a very good agreement between theory and experiment can be stated which reveals the importance of the distortion of atomic states by the long range Coulomb interaction.

Since for a detailed test of capture theories it is desirable to identify the capture cross-sections for the individual projectile states, the x-ray emission following electron capture has been measured in addition [5]. Figure 2 shows sample coincident x-ray spectra recorded at an observation angle of 132° in coincidence with down-charged U^{91+} ions for $U^{92+} \rightarrow N_2$ collisions. The spectra show x-ray radiation corresponding to REC into the empty K and higher shells as well as the characteristic Lyman and Balmer lines. Simultaneously, as the projectile energy decreases, the Doppler shifted characteristic Lyman $\alpha_{1,2}$ transitions (Lyα_1: $2p_{3/2} \rightarrow 1s_{1/2}$; Ly$\alpha_2$: $2p_{1/2}, 2s_{1/2} \rightarrow 1s_{1/2}$) become more intense and exhibit a strong change of the relative intensities of the Lyα_1 and Lyα_2 components.

A. State Selective Capture Studies: Balmer Transitions of Hydrogen-Like Uranium

Until now, no final state selective information about electron capture was available in the domain of intermediate and fast collisions. For high-Z ions, however, the spectroscopic studies of *n,l,j*-sensitive population cross-sections are accomplished by the large fine-structure splitting present. The latter allows us to obtain population cross-sections for specific projectile states from the measured Balmer transitions produced by electron capture. In Fig. 3 the Balmer spectrum of H-like uranium recorded for fast $U^{92+} \rightarrow N_2$ collisions at 358 MeV/u (upper spectrum) is compared with the one obtained for the same collision system but at the energy of 49 MeV/u (bottom spectrum). In addition, the most prominent x-ray lines in the spectra are marked by arrows, explaining the origin of the various x-ray lines. Contrary to the spectrum measured at the high energy (see upper spectrum in Fig. 3), which is governed by $\ell \rightarrow \ell + 1$ ($s \rightarrow p$ transitions, see dotted arrows in Fig. 3), the dominant transitions observed for the decelerated ion stem from atomic levels with angular momenta $\ell \geq 1$ (see solid arrows in Fig. 3). This distinct difference must again be attributed to the role of the two different population mechanisms, REC and NRC.

In order to compare the experimental data with capture theories, a spectrum simulation was performed [22]. At the high energy, the simulation considers only the REC process by the application of rigorous relativistic calculations. For the decelerated ions, where the NRC process is most important, the post version of the eikonal approach [18] was considered in addition as well as the CDW approach [19]. All projectile shells up to n=20 were taken into account in order to describe the high energy part of the spectra where transitions from Rydberg levels are located. Moreover, exact relativistic transition rates were considered. It is interesting to note that both theories applied for NRC predict very similar final n, l-distributions and therefore give almost identical Balmer spectra. For the energy of 68 MeV/u, the theoretical spectrum is represented by the shaded area given in the bottom spectrum of Fig. 3, which appears to describe well the experimental one. This good agreement obtained confirms the eikonal (post version) and the CDW predictions: At the two lowest beam energies of 49 MeV/u and 68 MeV/u, a broad n_f-distribution with a maximum at $n_{max} = 4$ exists whereby final angular momentum states with $\ell_{max} = n_{max} - 1$ are favored. However, one deficit of the eikonal approach gets obvious. Whereas, the higher potential prescription had to be applied in order to reproduce the total cross-section data, only the post-version was found to describe correctly the exclusive cross-section data derived from the x-ray spectra. In contrast, the higher potential prescription yields a similar n, l-distribution as obtained from the OBK-theory, an approach where the distortion of atomic states by the long-range Coulomb interaction is neglected. The latter is known to overestimate considerably (up to a factor of ten) total cross-section data, however, it is still commonly used in order to predict the n,l-distribution for NRC. For the case of $U^{92+} \rightarrow N_2$ at 49 MeV/u and 68 MeV/u, the theoretical spectra obtained from the inclusion of the OBK theory are in strong variance with the experimental data [22]. This shows, that Coulomb distortion effects have also a considerable influence on the relative n, l, j-distribution for non-radiative electron capture.

B. Angular Distribution and Alignment Investigations for the Time-Reversed Photoionization Process

Photoionization is one of the most important interaction processes between radiation and matter [23]. Recently, it has been proposed that the study of its time reversed analog which occurs in ion-atom collisions, i.e. of REC, can be applied for the investigation of the atomic photoeffect, in particular, in the domain of high-Z ions [21,24,25] where the photon-atom interaction is influenced by relativistic effects. For the exploration of such details, angular distributions provide a very sensitive probe [26]. At high-Z the full retarded multipole expansion of the photon field must be considered and the strength of relativistic effects may lead to considerable corrections [27]. Evidently, the latter effects are of particular interest when dealing with high-Z ions.

With the new target chamber at the ESR gas-jet complete angular distribution studies are now accessible for the first time. Here, various observation angles starting from nearly 0° up to 180° are available which were used recently for a first experimental angular distribution study of K-REC into a high-Z ion, aiming at an identification of spin-flip contributions. As has been theoretically predicted [14,15], such magnetic transitions are of considerable importance for high projectile charges, leading to photon emission even at 0°. Since for *spinless* electrons, the latter is forbidden by angular conservation laws, this provides a unique signature for spin-flip transitions in relativistic ion-atom collisions.

In the experiment the K-REC radiation was observed for U^{92+} ions colliding at an energy of 310 MeV/u with a molecular nitrogen target and by using various Ge(i) and NaI x-ray detectors at in total six different observation angles [28]. At nearly 0°, a segmented Ge(i) detector was used, mounted on a step-motor driven device. This detector was moved to its final position after the ion stacking procedure was finished. In its final position the observation angle amounts to 4.6°. In Fig. 4, an x-ray spectrum recorded by this detector is displayed, obtained from a preliminary data analysis, where the K-REC transitions show up clearly at the very high energy of about 660 keV. The occurrence of the K-REC line at nearly 0° allowed us for the first time to identify spin-flip transitions occurring in relativistic ion-atom collisions.

By means of REC, photoionization can also be studied for excited states in high-Z H-like ions [21]. In the following, we consider the inverse of a two-photon/one-electron ionization process. Here, the first photon resonantly excites an electron from the $1s_{1/2}$ ground state into the $2p_{3/2}$ hydrogen-like state and subsequently the second photon ionizes the excited electron within the lifetime of the $2p_{3/2}$ state, i.e. for the case of H-like uranium a time of the order of 10^{-17} s. We are interested in the magnetic subshell population of REC into the $2p_{3/2}$ state. Usually, information about degenerate atomic states, which differ only in their magnetic quantum number, is obtained by polarization measurements. However, since for high-Z ions, like uranium, the Lyα_1 transition energy appears close to 100 keV, a polarization measurement is almost impossible. The alignment of the $2p_{3/2}$ state and consequently its magnetic- substate population can also be deduced from an angular distribution measurement. Since the $2p_{3/2}$ decays by an **E1** transition to the ground state, the anisotropic emission in the emitter frame is simply given by [29]

$$I(\theta) \propto 1 + \beta_A \cdot [1 - \frac{3}{2}\sin^2\theta] \tag{3}$$

where θ denotes the emission angle in the projectile frame and β_A gives the coefficient of the alignment which is related to the population cross-sections $\sigma(j, m_j)$ for the magnetic sublevels [29]

$$\beta_A = \frac{1}{2} \cdot \frac{\sigma_{(3/2,3/2)} - \sigma_{(3/2,1/2)}}{\sigma_{(3/2,3/2)} + \sigma_{(3/2,1/2)}} \tag{4}$$

Consequently, by measuring the Lyα_1 emission at only a few observation angles, the relative population of the magnetic sublevels can be experimentally determined.

Such investigations were performed recently with bare Pb^{82+} and U^{92+} projectiles at the gas-jet target of the ESR storage ring [21]. In order to reduce possible systematic uncertainties, we took advantage of the close spaced, simultaneously observed Lyα_2+**M1** transitions, which are isotropic in the emitter frame. By normalization to the latter, almost all systematic uncertainties cancel out. Moreover, in order to control possible cascade population of the $2p_{3/2}$ state, also the Balmer spectra were recorded (see Fig. 3). All prominent lines in the cascade spectra were identified as originating from $j = 1/2$ states (see transition assignment given in the Fig. 3). Therefore, no alignment is introduced by cascades. From the measured alignment of the $2p_{3/2}$-levels follows, that about 75% of the capture events populate the $|m_j|$=1/2 sublevels of the $2p_{3/2}$ state which corresponds to a 40% linear polarization of the emitted Lyα_1 radiation. By subtracting the cascade contribution, we were able to deduce that direct radiative capture into the $2p_{3/2}$ state populates the $|m_j|$=1/2 magnetic sublevels by more than 90%. As a consequence, a surprisingly strong linear polarization by as much as 50% can be infered from this finding. This result was derived from measurements at only three observation angles, exploiting the fact that the shape of the angular distribution is precisely known (see Eq. 3). During the last experiment with the new target chamber, however, we obtained also data for the alignment of the $2p_{3/2}$ in H-like uranium, by a measurement in the angular range between nearly 0° and 150° ($U^{92} \rightarrow N_2$ collisions at 310 MeV/u). In Fig. 5, the measured intensity distribution of the Lyα_1 radiation is depicted as function of the observation angle. In addition, the solid line depicts a least square fit of Eq. 3 to the experimental data points. As a result, we obtain an β_A parameter of 0.225 $\pm$ 0.017, in accordance with the former experimental findings [21]. However, all experimental alignment data appear to be in variance with complete theoretical *ab initio* calculations [29,30]. Note, that for comparison between experimental and theoretical results, the theoretical data had to be corrected for the cascade population of the $2p_{3/2}$ state. Although the latter had been measured, it might be responsible for the found deviations. Another reason could be the **M2** decay branch of the $2p_{3/2}$ level. In uranium it contributes by about 3% to the total decay probability but may interfere with the dominant **E1** transition. So it may alter both, the shape of the angular distribution on one hand and the size of the β_A parameter on the other hand. Further investigation are required in order to elucidate this topic.

III. SUMMARY

In summary, an overview on the current status of atomic collision experiments at the storage ring ESR was given. The experiments discussed concentrate on electron capture studies into decelerated and highly relativistic high-Z ions at the jet-target of the ring by means of x-ray spectroscopy. Due to the large fine structure splitting and the reduced Doppler broadening at the low beam energies, this allowed us to obtain precise $n_{n,l,j}$-selective information about electron transfer into high-Z projectiles and to reveal the importance of Coulomb distortion effects by comparison with capture theories presently available. At the high energies, magnetic effects induced by the relativistic motion and the strong field of the projectile were addressed by the experimental investigations. Here, a first complete angular differential study of K-shell REC into a bare high-Z ion was conducted. In particular, the observation of photon emission close to 0° allowed us to identify for the first time spin-flip contributions to the differential cross sections. In this way, the electron spin manifests itself in a particularly clear-cut manner as it was theoretically predicted recently. Such investigations give at the same time experimental access to its time reversed process, i.e. it allows to obtain experimental information about the otherwise inaccessible photoionization process of hydrogenlike high-Z ion. This could also be demonstrated by our study of the time-reversed two-step photoionization process, where REC is a production process of strongly polarized Lyα_1-radiation. This finding underlines the importance of the REC process for the study of photoionization in the domain of high-Z one- and few-electron ions.

ACKNOWLEDGMENT

This work was done in collaboration with F. Bosch, R.W. Dunford, A. Krämer, C. Kozhuharov, T. Ludziejewski, P.H. Mokler, Z. Stachura, P. Swiat, A. Warczak and with the members of the ESR team, K. Beckert, B. Franzke, H. Reich, F. Nolden, and M. Steck. The author would like to thank J. Eichler for the close collaboration over many years and his continuous support with new and stimulating theoretical results.

---

[1] F. Bosch, in: *The Physics of Electronic and Atomic Collisions*, AIP Conference Proc. 295, eds.: T. Andersen, B. Fastrup, F. Folkmann, H. Knudsen, N. Andersen, New York 1993, p. 3.

[2] K. Blasche, B. Franzke, *Proc. of the 4^{th} Europ. Part. Acc. Conf.*, V. Suller and Ch. Petit-Jean-Genaz eds., World Scientific, Singapore, 1994, 133–137.

[3] P.H. Mokler and Th. Stöhlker, Adv. in Atomic, Molecular, and Optical Physics, Vol.37, 297 (1996).

[4] H. Reich, W. Bourgeois, B. Franzke, A. Kritzer, and V. Varentsov, Nucl. Phys. A**696**, (1997).

[5] Th. Stöhlker et al., Phys. Rev. A **58**, 2043 (1998).

[6] A. Krämer et al., see contribution to this conference (1998).

[7] T. Ludziejewski et. al., Nucl. Instr. Meth. in print (1998).

[8] T. Ludziejewski et al., J. Phys. B **31**, 2601, (1998).

[9] A. Warczak et al., Nucl. Instr. Meth. B **98**, 303 (1995).

[10] J.R. Oppenheimer, Nucl. Phys. **31**, 349 (1928).

[11] J. Eichler and W.E. Meyerhof *Relativistic Atomic Collisions* (Academic Press, San Diego, 1995).

[12] C. Scheidenberger et al., Nucl. Instr. and Methods B **142**, 441 (1998).

[13] M. Stobbe, Ann. Phys. 7, 661 (1930).

[14] A. Ichihara, T. Shirai, and J. Eichler, Phys. Rev. A **49**, 1875 (1994).

[15] J. Eichler, A. Ichihara, and T. Shirai, Phys. Rev. A **51**, 3027 (1995).

[16] Th. Stöhlker et al.,Phys. Rev. A**51**, 2098 (1995).

[17] J. Eichler, Phys. Rev. A**32**, 112 (1985).

[18] J. Eichler, Phys Rep. **193**, 165 (1990).

[19] Dz. Belkic, R. Gayet, A. Salin, Comp. Phys. Comm. **23**, 153 (1981).

[20] Th. Stöhlker et al., Hyperfine Interactions **108**, 29 (1997).

[21] Th. Stöhlker et al., Phys. Rev. Lett. **79**, 3270 (1997).

[22] Th. Stöhlker et al., to be published.

[23] For a summary of the atomic photoeffect, see, e.g., R.H. Pratt, A. Ron, and H.K. Tseng, Rev. Mod. Phys. **45** 273 (1973).

[24] A. Ichihara, T. Shirai, and J. Eichler, Phys. Rev. A **54**, 4954 (1996).

[25] Th. Stöhlker, P.H. Mokler, C. Kozhuharov, A. Warczak, Comments At. Mol. Phys. 33(5), 271

(1997).

[26] A.F. Starace, in *Corpuscles and Radiation in Matter I* edited by W. Mehlhorn, Handbuch der Physik **31**, 1 (Springer Verlag, Berlin 1982).

[27] B. Craseman, X-Ray and Inner-Shell Process 1996 (AIP, Woodbury, New York, 1997), p. 3.

[28] Th. Stöhlker et al.,in preparation for Phys. Rev. Lett. .

[29] J. Eichler, Nucl. Phys. A **572**, 147 (1994).

[30] J. Eichler, A. Ichihara, T. Shirai, Phys. Rev. **58**, 2128 (1998).

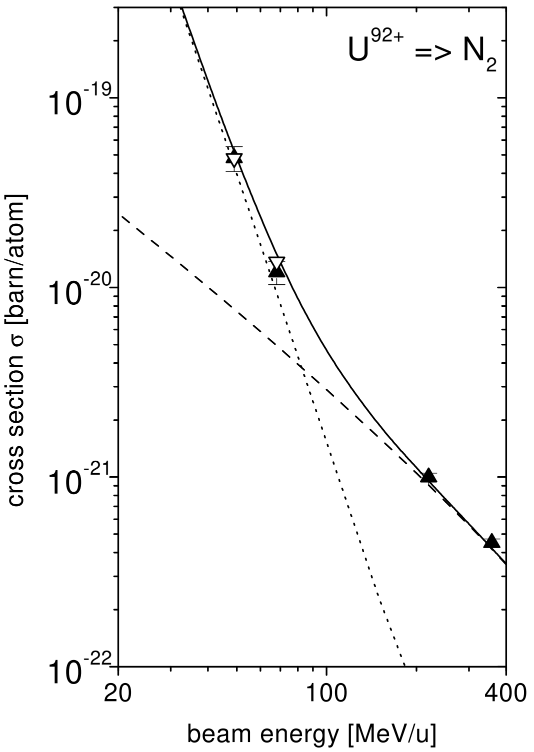

FIG. 1. Total electron-capture cross sections for U^{92+} on a N_2 target versus projectile energy [5]. The dotted line represents the result of the eikonal approach for the NRC process [17,18] whereas the REC cross-sections [13] are depicted by the dashed line. The solid line refers to the sum of both predictions. The sum of CDW [19] and REC calculations is given by the open triangles.

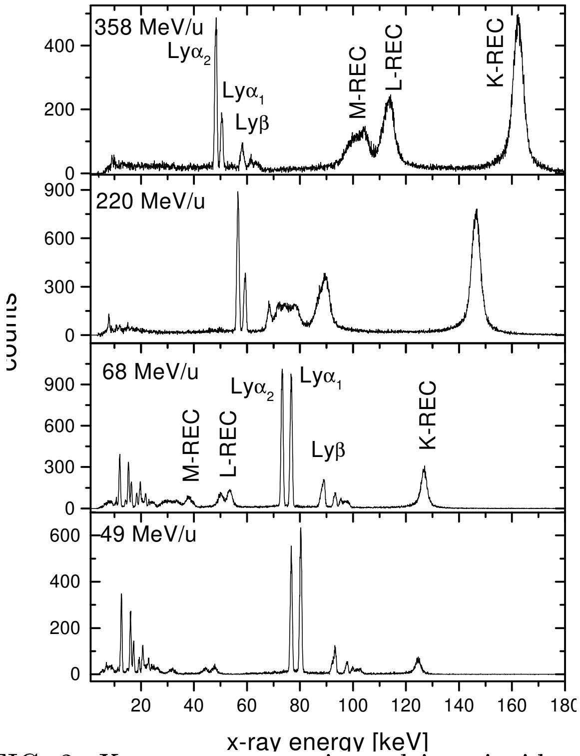

FIG. 2. X-ray spectra registered in coincidence with the particle counter for 49, 68, 220, and 358 MeV/u U^{92+} interacting with a N_2 target. The spectra (laboratory frame) were measured at the observation angle of 132° [5].

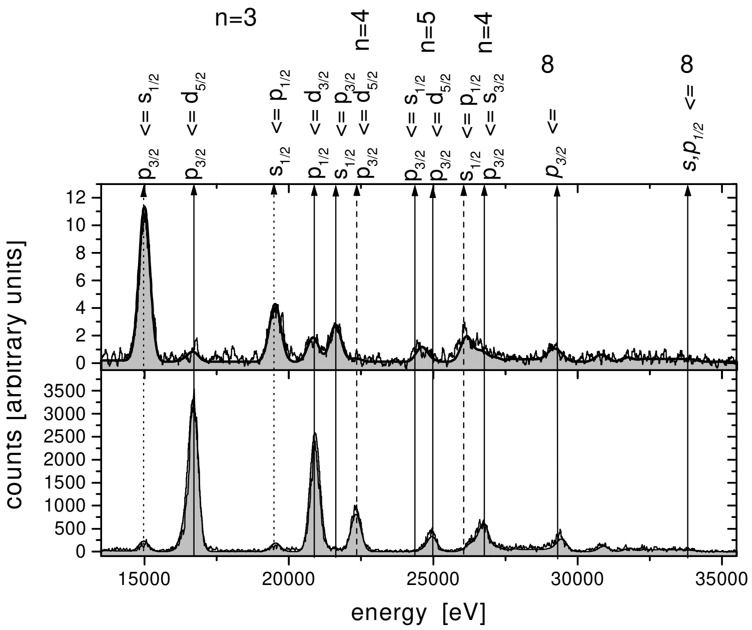

FIG. 3. Balmer spectrum of U^{91+} measured in coincidence with electron capture for $U^{92+} \rightarrow N_2$ collisions [20]. Spectrum at the top: 358 MeV/u [21]; Lower spectrum: 68 MeV/u. The shaded area depict the results of a spectrum simulation (compare text).

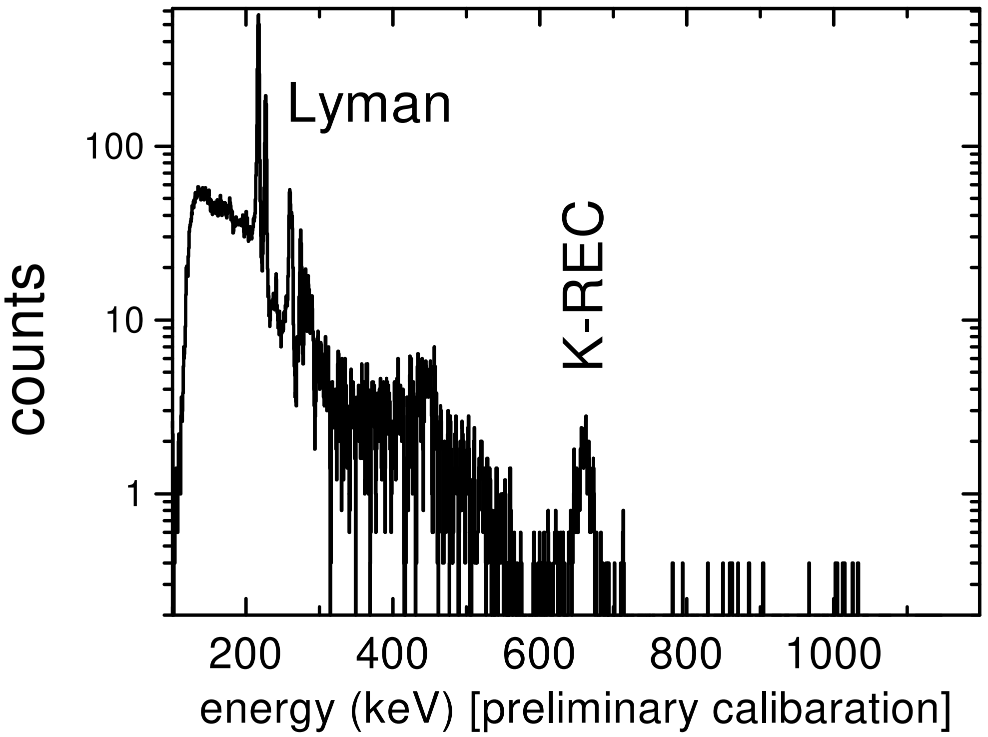

FIG. 4. X-ray spectrum measured at nearly 0° for $U^{92+} \rightarrow N_2$ collisions at 310 MeV/u [5].

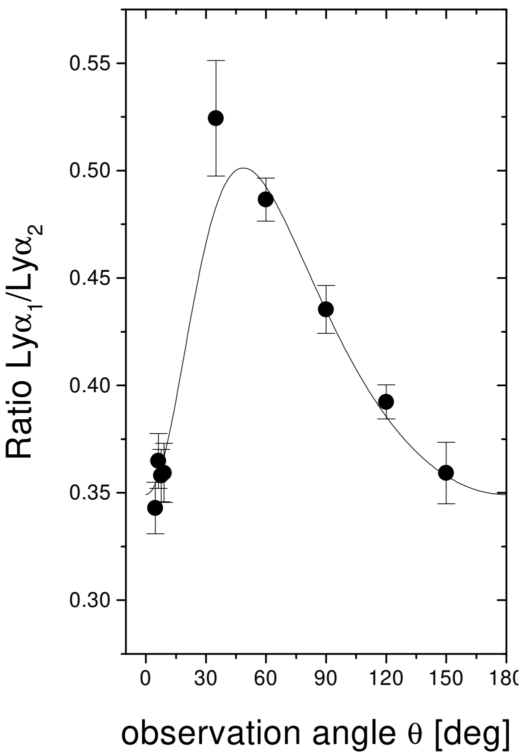

FIG. 5. Experimental Lyα_1/Lyα_2 intensity ratio as function of the observation angle (soild squares), measured for 310 MeV/u $U^{92+}\rightarrow N_2$ collisions. The solid line depicts the result of the least square adjustment of Eq. (3) to the experimental data.